Multiphysics Modeling and Simulation of a Solid Oxide Electrolysis Cell

D. Grondin[*,1], J. Deseure[1], A. Brisse[2], M. Zahid[2] and P. Ozil[1]
[1]Laboratoire d'Électrochimie et de Physico-chimie des Matériaux et des Interfaces (LEPMI), UMR 5631 CNRS-INPG-UJF, [2]European Institute for Energy Research (EIFER)
*Corresponding author: LEPMI, BP 75, 38402 Saint Martin d'Hères, France, dominique.grondin@lepmi.inpg.fr

Abstract: Based on solid oxide fuel cell (SOFC) technology, solid oxide electrolysis cell (SOEC) offers an interesting solution for mass hydrogen production. This study proposes a multiphysics model to predict the SOEC behavior, based on similar charge, mass and heat transport phenomena as for SOFC. However the mechanism of water steam reduction on Nickel/Yttria Stabilized Zirconia (YSZ) cermet is not yet clearly identified. Therefore a global approach and several electrochemical kinetic equations were used for modeling. The simulated results demonstrated that a Butler-Volmer's equation including concentration overpotential provides an acceptable estimation of the experimental electric performance. These simulations highlighted three thermal operating modes of SOEC and showed that temperature distribution depends on gas feeding configurations.

Keywords: hydrogen production, solid oxide electrolysis cell, multiphysics modeling, diffusion phenomena, electrochemical kinetic description

1. Introduction

Recently, significant research efforts are achieved to develop hydrogen economy. Hydrogen is a promising energy carrier due to its abundance, mainly in water, the high value of released energy (120 MJ/kg) and the absence of greenhouse gas emissions after combustion. Contrary to fossil fuels, hydrogen does not exist in a native state and so its use requires its production. Nowadays, the industrial mass production of hydrogen is mainly based on hydrocarbons reforming. However water electrolysis could be the most convenient production process if it uses a clean renewable energy source. From a thermodynamical point of view, water electrolysis is more interesting at higher temperature because of a lower electricity demand. Based on the Solid Oxide Fuel Cell (SOFC) technology, a Solid Oxide Electrolysis Cell (SOEC) is a device that allows electrochemical water splitting at high temperature (700 – 900°C). The cell consists on the assembly of a three-layer region involving two ceramic electrodes separated by a dense ceramic electrolyte made in the same materials as for a SOFC (Fig. 1).

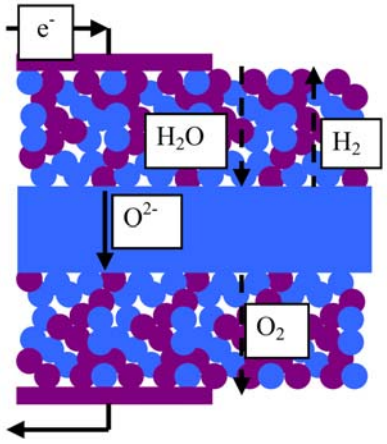

Figure 1. Schematic view of a SOEC

The hydrogen electrode is usually composed of nickel and yttrium stabilized zirconia (YSZ) cermet. The electrolyte is made of YSZ and the oxygen electrode is based on perovskite-type oxides, which is usually strontium-doped lanthanum manganite $La_{1-x}Sr_xMnO3$ (LSM). The electrochemical reactions in SOEC electrodes are as it follows:

Cathode: $H_2O + 2e^- \rightarrow H_2 + O^{2-}$ (1)

Anode: $O^{2-} \rightarrow ½\ O_2 + 2e^-$ (2)

At cathode, water steam is reduced and oxygen ions are produced (1). Then, oxygen ions migrate through the electrolyte to the anode where oxygen molecules and electrons are released (2). So, the ionic and electronic currents produced and consumed at electrodes cross the whole SOEC and generate heat sources due to the internal cell resistance. If the cell voltage value is $\Delta H/nF$, the heat source exactly provides the heat removed by the steam electrolysis process

(thermo neutral voltage). For upper and lower cell potential values, the operating modes are respectively endothermic and exothermic ones.

The first works devoted to SOEC were mainly experimental ones and were carried out in the 80's in a context of a relevant decline in oil production. However these studies have been suspended until the recent development of SOFC and the investigation of reversible SOFC. Many computing studies showed a great relevance for understanding and optimizing SOFC [1]. Computation fluid dynamics model is a quite recent method to investigate the SOEC stack behavior. Most of SOEC models are based on models previously developed for SOFC. Indeed, a 3-D SOEC model was already developed in order to investigate the effects of operating conditions on current densities and temperature distributions. Nevertheless, few works are available by literature regarding the water reduction kinetic on Nickel/YSZ cermet. Some experimental studies were carried out and corresponding reaction mechanisms were suggested but no further studies confirmed these proposals.

More recently, two electrochemical models were developed for an electrolyte supported cell and simulations were compared to experimental data. Both models seem to provide quite accurate predictions although there are different. Only one theoretical study was proposed for a cathode-supported SOEC, but without any comparison with experimental data. The major part of available models uses a Butler-Volmer's law for activation overpotential calculation. However this approach seems to be not precise enough since some earlier studies demonstrate that several chemical and electrochemical steps should occur.

This study proposes a multiphysics model of a single SOEC. Several electrochemical kinetic laws are used to predict the electric behavior of the cell under study. The Butler-Volmer law pertinence is discussed for different operating conditions. Finally, the effect of feeding configuration on temperature distribution is presented.

2. Nomenclature

A Specific surface area (m^2/m^3)
b Tafel slope (V)
c Concentration (mol/m^3)
Cp Heat capacity (J/mol)
d Mean diameter (m)
D Diffusion coefficient (m^2/s)
F Faraday constant (96485 C/mol)
j Electrochemical current density (A/m^2)
J Total current density (A/m^2)
j_0 Exchange current density (A/m^2)
K Permeability (m^2)
M Molecular weight (kg/mol)
p Pressure (Pa)
R Universal gas constant (8.314 J/mol/K)
S Current source (A/m^3)
V Potential (V)
T Temperature (K)
u Gas velocity (m/s)
y Molar fraction (-)

Greeks letters

α Charge transfer coefficient (-)
Γ Reaction rate ($mol/m^3/s$)
ΔS Water entropy formation (J/mol/K)
ε Porosity (-)
η Overpotential (V)
κ Thermal conductivity (W/m/K)
μ Gas viscosity (Pa.s)
ρ Gas density (kg/m^3)
σ Conductivity (S/m)
τ Tortuosity (-)
Φ Heat source (W/m^3)

Subscripts

a Anode
atm Atmospheric
c Cathode
d Darcy
e Electrolyte
el Electric
eq Equivalent
g Grain
H_2 Hydrogen
H_2O Water
i,j Binary coefficient of species *i,j*
i,k Knudsen coefficient of species *i*
io Ionic
i,0 Bulk concentration of species *i*
N_2 Nitrogen
o Operating temperature
ox Oxidant species
O_2 Oxygen
p Pore
red Reductive species
TBP Triple Phase Boundary
0 Inlet condition

Superscripts

eff Effective

3. Governing equations

The physical phenomena taking place within a SOEC were separately studied. Model accuracy depends on the selected mathematical description. SOFC and SOEC are roughly similar system. As a first step, the mathematical model developed for SOFC can be used for SOEC because of the similitude of both systems. The multiphysics approach takes into account dependence between phenomena. The main assumptions concern gas velocities along the gas channels, electrodes ionic conductivities and material thermal conductivities that are all supposed to stay constant.

3.1 Charge balance

SOEC electrodes are mixed electronic-ionic conductors. The transport of each type of charge particle (e^-, O^{2-}) is described by an Ohmic's law expressed as:

$$-\nabla.(\sigma_i \nabla V_i) = S_{i,a,c} \quad (3)$$

S being the current source term defined by relation (4).

$$S_{i,a,c} = \pm A_{TPB} j_{a,c} \quad (4)$$

The electrochemical reaction is assumed to take place at the triple phase boundary (TPB) i.e. the contact area between gas, electric and ionic conductors. The specific surface area (A_{TPB}) is the surface generated by these contact areas in the electrode volume. TPBs are assumed to be uniformly distributed in the electrode volume. For simulations, A_{TPB} will be included in the exchange current density value. In the same electrode, current source related to anion consumption/production is the opposite of that for electron (5).

$$S_{el} = -S_{io} \quad (5)$$

In the electrolyte, no current source term is considered and a pure ionic conductivity is assumed. Electrodes electric and electrolyte ionic conductivies are considered as temperature dependent.

3.2 Mass balance

Mass transport is mainly driven by diffusion – convection in the whole cell and can be described by:

$$\nabla.(-D\nabla c) = -u.\nabla c + \Gamma \quad (6)$$

this expression differing according to the considered part of the cell.

3.2.1 Hydrogen side

In the case under study, water steam is provided with hydrogen and nitrogen at cathode side. Stefan-Maxwell diffusion model is used regarding the significant difference between molecular weight of species. Moreover, Knudsen diffusion should be considered in the electrode that is a porous media. Thus, the dusty-gas model (DGM) is used at cathode. Such model seems to provide the most accurate description of mass transport for SOFC anode [2]. The DGM may be summarized in the following equivalent effective diffusion coefficient [2]:

$$D_{eq}^{eff} = \frac{1}{D_{H_2O,k}} + \frac{1}{D_{H_2O,N_2}^{eff}} + (1-y_{N_2})\left(\frac{1}{D_{H_2O,H_2}^{eff}} - \frac{1}{D_{H_2O,N_2}^{eff}}\right) \quad (7)$$

$$-\frac{\beta y_{H_2O}}{D_{H_2O,H_2}^{eff}}$$

$$\text{with } \beta = 1 - \left(\frac{M_{H_2O}}{M_{H_2}}\right)^{1/2} \quad (8)$$

The Knudsen diffusion coefficient of the species *i* ($D_{i,k}$) is calculated from relation (9)

$$D_{i,k} = d_p \frac{\varepsilon}{3\tau}\sqrt{\frac{8RT}{\pi M_i}} \quad (9)$$

while the mean pore diameter is determined considering electrode characteristics (10).

$$d_p = \frac{2}{3}\frac{\varepsilon}{1-\varepsilon} d_g \quad (10)$$

Where the effective diffusion coefficient is the diffusion coefficient in a porous media. Different models were used to obtain a good estimation of this coefficient [3]. The models developed for SOFC or SOEC generally use the following formula [1]:

$$D_{i,j}^{eff} = \frac{\varepsilon}{\tau} D_{i,j} \quad (11)$$

where the water consumption rate (Γ_c) is derived from the Faraday's law (12).

$$\Gamma_c = -\frac{S_c}{2F} \quad (12)$$

In the hydrogen electrode, only diffusion is assumed to take place, because there is no increase of gas molar number. The permeation flux is null since the total pressure in the

electrode is constant (u=0) and diffusivity D in equation (6) is in fact D_{eq}^{eff} .

No Knudsen diffusion occurs within the gas channel, which is not a porous media. The equivalent diffusion coefficient is then expressed as it follows:

$$D_{eq} = \frac{1}{D_{H_2O,N_2}} + (1-y_{N_2})\left(\frac{1}{D_{H_2O,H_2}} - \frac{1}{D_{H_2O,N_2}}\right) - \frac{\beta y_{H_2O}}{D_{H_2O,H_2}} \quad (13)$$

Gas velocity (u) is assumed to be constant along the channel. There is no reaction (Γ=0) and $D=D_{eq}$. All diffusion coefficients used in this model are considered as temperature dependent.

3.2.2 Oxygen side

In the oxygen electrode, oxygen molecules are produced according the following reaction rate:

$$\Gamma_a = \frac{S_a}{4F} \quad (14)$$

Total pressure in this electrode increases and consequently a permeation flux has to be computed. Gas velocity in the anode (u_a) is given by the Darcy's law (15). Gas viscosity (μ) is here dependent on both composition and temperature. Electrode permeability (K) is determined by the Kozeny-Carman relation (16) and the oxygen effective diffusion coefficient is calculated owing to the Bosanquet formula (17). In the anode domain, we consider that $D=D^{eff}$.

$$u_a = -\frac{K}{\mu}\nabla p \quad (15)$$

$$K = \frac{\varepsilon^3}{72\tau(1-\varepsilon)^2} d_g^{\,2} \quad (16)$$

$$D^{eff} = \left(\frac{1}{D_{O_2,N_2}^{eff}} + \frac{1}{D_{O_2,k}}\right)^{-1} \quad (17)$$

In the gas channel, no reaction occurs (Γ=0) and the gas velocity is assumed to be constant. A Fick's diffusion model is used since difference between molecular weight of species is not really significant ($D=D_{O_2,N_2}$).

3.3 Heat balance

Temperature is a key parameter in such system due to the dependence of many parameters on it. Moreover, materials are really sensitive to temperature gradient. While SOEC operates at high temperature, 800°C in the present case, radiative heat transfer becomes non-negligible. However, a previous study demonstrated that radiative heat transfer inside the cell could be neglected ahead of conductive transfer for a SOFC [4]. Then, only convection and conduction phenomena are taken into account to describe heat transfer in the cell under study. Heat balance can be expressed as:

$$\nabla.\left(-\kappa\nabla T + \rho C_p T u\right) = \Phi \quad (18)$$

Gas physical properties depend on both composition and temperature. Solids thermal conductivities are constant. The heat source (Φ) varies according to the considered part of the cell. Electrochemical reaction irreversibilities are considered in addition to the Joule's effect in the electrodes, (19, 20). An ionic Joule's effect only occurs in the electrolyte (21) and there is no heat source in the gas channels.

$$\Phi_c = \left(\frac{-T\Delta S}{2F} + \eta\right)S_c - \mathbf{J}_c.\nabla V_{el} - \mathbf{J}_c.\nabla V_{io} \quad (19)$$

$$\Phi_a = \eta S_a - \mathbf{J}_a.\nabla V_{el} - \mathbf{J}_a.\nabla V_{io} \quad (20)$$

$$\Phi_e = \mathbf{J}_e.\nabla V_{io} \quad (21)$$

3.4 Charge transfer models

The electrochemical current density (j) is a relevant variable since it acts in all balances and it is linked to electrochemical reaction kinetic data. There is a poor literature about water steam reduction kinetic on Nickel/YSZ cermet. It is thus difficult to have an accurate expression for j. However, different models exist for current density calculation from overpotential that is expressed here by is given by relation (22). In this study, various expressions were used to simulate the electric cell performance: the very simple Tafel's law (23) and Butler-Volmer's law without (24) and with concentration overpotential (25):

$$\eta = V_{el} - V_{io} \quad (22)$$

$$j = j_0 \exp\left(\frac{\eta}{b}\right) \quad (23)$$

$$j = j_0\left(\exp\left(\frac{2\alpha F\eta}{RT}\right) - \exp\left(\frac{-2(1-\alpha)F\eta}{RT}\right)\right) \quad (24)$$

$$j = j_0\left(\frac{c_{red}}{c_{red,0}}\exp\left(\frac{2\alpha F\eta}{RT}\right) - \frac{c_{ox}}{c_{ox,0}}\exp\left(\frac{-2(1-\alpha)F\eta}{RT}\right)\right) \quad (25)$$

4. Numerical Model

The mathematical model previously defined is solved using the code of COMSOL Multiphysics. Obviously geometry and boundary conditions have to be defined before solving the set of partial differential equations and performing simulations with the software.

4.1 Geometry and mesh

This study aims to investigate only the behavior of the cell that is here is a single circular SOEC. The geometry will thus only include electrodes, electrolyte and gas channels. Only a cross-section of the cell along the radius is modeled due to symmetry (Fig. 2). The cell dimensions and characteristics are gathered in Table 1.

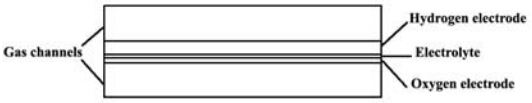

Figure 2. Geometry for modeling

A mapped mesh is used to obtain a reasonable number of degrees of freedom allowing calculation convergence within an acceptable time. All simulation results are obtained using the predefined mapped mesh named as *extremely fine*. The number of degrees of freedom is here 26 733 and the minimum element quality is 0.0359.

Table 1: Main cell characteristics

Cathode thickness (m)	240.10^{-6}
Electrolyte thickness (m)	7.10^{-6}
Anode thickness (m)	20.10^{-6}
Cell radius (m)	39.10^{-3}
Electrodes porosity (-)	0.3
Anode tortuosity (-)	1.7
Cathode tortuosity (-)	6
Electrodes mean grain diameter (m)	10.10^{-6}

4.2 Boundary Conditions

This section presents the boundary conditions used to solve each balance. Boundaries can be located in Figure 3.

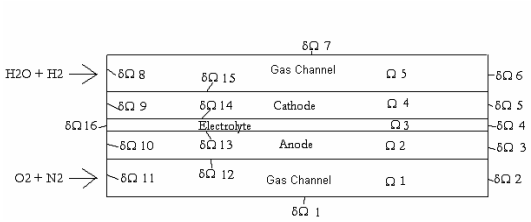

Figure 3. Schematic view of the boundary domain

The present multiphysics problem uses six equations needing boundary conditions for solving. All non-insulated boundaries are gathered in the following table.

Table 2. Non-insulated boundary conditions

Balance	δΩ	Type	Expression
Electric	12	Potential	V_a
Electric	15	Potential	V_c
Darcy	12	Pressure	p_{atm}
Darcy	13	Outflow	$JM_{O_2}/4F\rho$
Water	8	Concentration	$c_{H_2O,0}$
Water	6	Convective flux	-
Oxygen	11	Concentration	$c_{O_2,0}$
Oxygen	2	Convective flux	-
Heat	8, 11	Temperature	T_o
Heat	2, 6	Convective flux	-

A parametric solver is used with the potential applied at the oxygen electrode (V_a) as the parameter. The linear system solver is here *Direct PARDISO*.

5. Results and discussion

5.1 Charge transfer model accuracy

Simulations are performed with the three different expressions of the faradic current density given by the equations (23), (24), (25). A comparison with experimental polarization curves (cell potential vs. current density) obtained under steady-state conditions at 800°C is carried out to check the charge transfer model. The exchange current density and Tafel slope are tuned to fit the experimental polarization curves.

Figure 4 presents the best fits obtained from the three expressions. Description using a Tafel's law appears to be not accurate enough and is not suitable in our case. When the Butler-Volmer's law without concentration overpotential is used, a lower discrepancy is observed but the fitting

between simulated and experimental curves is not satisfactory. Only the Butler-Volmer's law including concentration overpotential provides a good prediction of the electric cell performance under the operating conditions (water molar fraction = 70%). This later model may be considered to be calibrated.

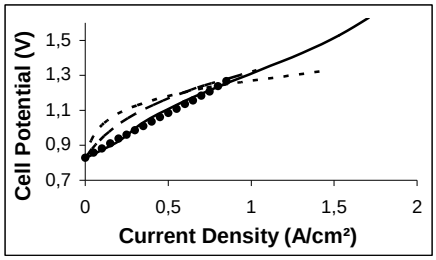

Figure 4. Comparison between simulated polarization curves using Tafel's law (---), Butler-Volmer's law without concentration overpotential (– –), Butler-Volmer's law with concentration overpotential (—) and the experimental one (●) for 70% inlet water molar fraction.

5.2 Influence of effective diffusion coefficient estimation

Before using the calibrated model to predict cell behavior in various operating conditions, it is necessary to check its predictive power for another inlet water partial pressure (30%). The model appears unable to predict the electric cell behavior as shown in Figure 5. Diffusion phenomenon seems to be critical at this concentration. As said previously, several laws are available for effective diffusion coefficient calculation. Bruggeman's law (30) is used to observe effective diffusion coefficient influence on simulation results.

$$D^{eff} = D\varepsilon^{\tau} \quad (30)$$

Tortuosity (τ) is an estimated parameter that is impossible to be properly determined with the cell under study. In some previous study, the tortuosity was considered as a tuning parameter to fit experimental data [1]. Here, the Bruggeman's law with a tortuosity set to 4.8 seems to be the most suitable law to describe diffusion phenomena in the cell (Fig. 5). A good agreement is then also observed with an inlet water molar fraction of 70% as shown by Figure 6.

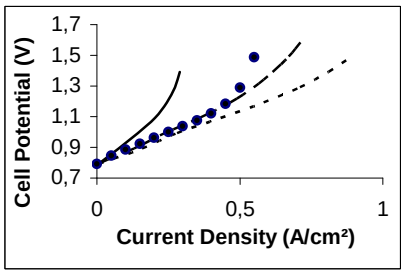

Figure 5. Comparison between simulated polarization curves using the Bruggeman's law with $\tau = 6$ (—), $\tau = 4.8$ (– –), the calibrated model (---) and the experimental polarization curve (●) for 30% inlet water molar fraction.

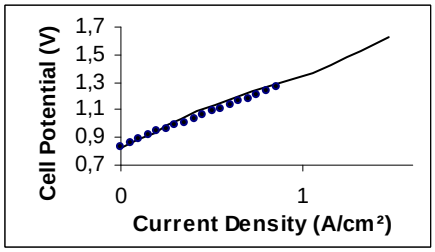

Figure 6. Comparison between simulated polarization curves using the Bruggeman's law ($\tau = 4.8$) (—) and the experimental one (●) for 70% inlet water molar fraction.

Porosity and mean grain diameter are estimated parameters having approximate values. Figure 7 shows the influence of these parameters on simulated polarization curves. Several values are used and in any case, a very good agreement between simulated and experimental curves is obtained. Observed difference may not be due to only diffusion phenomena description. Indeed, the Butler-Volmer's law assumes a single step electrochemical water reduction. Such assumption may be inadequate for low water steam partial pressure [5].

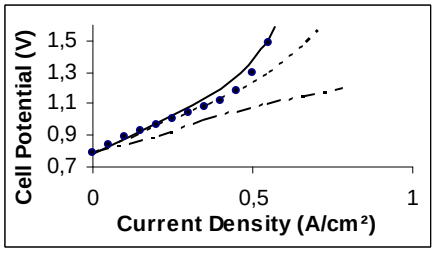

Figure 7. Comparison between simulated polarization curves with $\varepsilon = 0.3$ and $d_g = 10\mu m$ (---), $\varepsilon = 0.4$ and $d_g = 10\mu m$ (– · –), $\varepsilon = 0.3$ and $d_g = 6\mu m$ (—) and the

experimental one (●) for 30% inlet water molar fraction.

5.3 Influence of feeding configuration

A change in feeding configuration is investigated using the calibrated model for 70% inlet water molar fraction. Only oxygen flow direction has been changed to compute the counter-flow configuration. Concentration profiles and polarization curve appear to be similar in both configurations (not presented in this paper). The most interesting results concern temperature profile. As shown in Figure 8, temperature distributions are different according to feeding configuration. Another remarkable result is that three thermal behaviors are observed depending on the cell potential value. For a cell voltage lower than 1.3 V, a cooling effect is noted. Around 1.3 V, the cell and gases temperature is quite constant while it increases for higher potentials. This phenomenon is due to the endothermic water splitting reaction. At a critical value of cell potential (thermoneutral voltage), the Joule's effect heat source compensates the reaction heat consumption. Temperature is then constant (thermoneutral mode). Figure 9 shows temperature profiles in exothermal mode i.e. for cell potential higher than 1.3 V in both configurations.

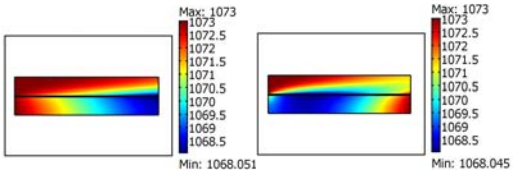

Figure 8. Temperature profile in a co- (a) and a counter-flow (b) configuration for a cell potential of 1.1V.

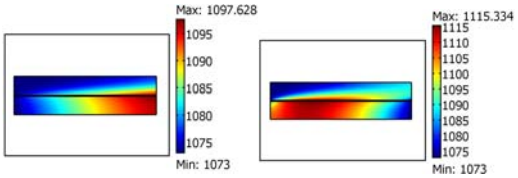

Figure 9. Temperature profile in a co- (a) and a counter-flow (b) configuration for a cell potential of 1.6V.

6. Conclusions

A multiphysics model of a solid oxide electrolysis cell has been developed and solved using COMSOL Multiphysics 3.4 software. Several electrochemical kinetic models have been used to investigate the most accurate one to predict the electric performance of the cell under study. The model using Butler-Volmer's law with concentration overpotential allows a good electric prediction for high inlet water partial pressure. For lower concentrations, a particular attention must be paid to the estimation of electrodes materials properties. Nevertheless, a more accurate electrochemical model for water reduction should be investigated to describe the high current density operation. The three thermal mode of SOEC have been observed in accordance with theory. Moreover, simulations showed that temperature distribution also depends on feeding configurations.

7. References

1. Yixiang Shi, Ningsheng Cai, Chen Li, Numerical modeling of an anode-supported SOFC button cell considering anodic surface diffusion, *Journal of Power Sources*, **164**, 639-848 (2007)

2. R. Suwanwarangkul, E. Croiset, M.W. Fowler, P.L. Douglas, E. Entchev, M.A. Douglas, Performance comparison of Fick's, dusty-gas and Stefan-Maxwell models to predict the concentration overpotential of a SOFC anode, *Journal of Power Sources*, **122**, 9-18 (2003)

3. Fun Gau Ho and William Strieder, Numerical evaluation of the porous medium effective diffusivity between the Knudsen and continuum limits, *The Journal of Chemical Physics*, **73**, 6296-6300 (1980)

4. D.L. Damm, A.G. Fedorov, Radiation heat transfer in SOFC materials and components, *Journal of Power Sources*, **143**, 158-165 (2005)

5. E.J.L. Schouler, M. Kleitz, E. Forest, E. Fernandez, P. Fabry, Overpotential of H_2-H_2O, Ni/YSZ electrodes in steam electrolyzers, *Solid State Ionics*, **5**, 559-562 (1981)